NASA/TM—2008-215475 AIAA–2008–4506

Preliminary Test Results of a Non-Contacting Finger Seal on a Herringbone-Grooved Rotor

Margaret P. Proctor and Irebert R. Delgado
Glenn Research Center, Cleveland, Ohio

November 2008

NASA STI Program . . . in Profile

Since its founding, NASA has been dedicated to the advancement of aeronautics and space science. The NASA Scientific and Technical Information (STI) program plays a key part in helping NASA maintain this important role.

The NASA STI Program operates under the auspices of the Agency Chief Information Officer. It collects, organizes, provides for archiving, and disseminates NASA's STI. The NASA STI program provides access to the NASA Aeronautics and Space Database and its public interface, the NASA Technical Reports Server, thus providing one of the largest collections of aeronautical and space science STI in the world. Results are published in both non-NASA channels and by NASA in the NASA STI Report Series, which includes the following report types:

- TECHNICAL PUBLICATION. Reports of completed research or a major significant phase of research that present the results of NASA programs and include extensive data or theoretical analysis. Includes compilations of significant scientific and technical data and information deemed to be of continuing reference value. NASA counterpart of peer-reviewed formal professional papers but has less stringent limitations on manuscript length and extent of graphic presentations.

- TECHNICAL MEMORANDUM. Scientific and technical findings that are preliminary or of specialized interest, e.g., quick release reports, working papers, and bibliographies that contain minimal annotation. Does not contain extensive analysis.

- CONTRACTOR REPORT. Scientific and technical findings by NASA-sponsored contractors and grantees.

- CONFERENCE PUBLICATION. Collected papers from scientific and technical conferences, symposia, seminars, or other meetings sponsored or cosponsored by NASA.

- SPECIAL PUBLICATION. Scientific, technical, or historical information from NASA programs, projects, and missions, often concerned with subjects having substantial public interest.

- TECHNICAL TRANSLATION. English-language translations of foreign scientific and technical material pertinent to NASA's mission.

Specialized services also include creating custom thesauri, building customized databases, organizing and publishing research results.

For more information about the NASA STI program, see the following:

- Access the NASA STI program home page at *http://www.sti.nasa.gov*

- E-mail your question via the Internet to *help@sti.nasa.gov*

- Fax your question to the NASA STI Help Desk at 301–621–0134

- Telephone the NASA STI Help Desk at 301–621–0390

- Write to:
  NASA Center for AeroSpace Information (CASI)
  7115 Standard Drive
  Hanover, MD 21076–1320

NASA/TM—2008-215475 AIAA–2008–4506

Preliminary Test Results of a Non-Contacting Finger Seal on a Herringbone-Grooved Rotor

Margaret P. Proctor and Irebert R. Delgado
Glenn Research Center, Cleveland, Ohio

Prepared for the
44th Joint Propulsion Conference and Exhibit
cosponsored by the AIAA, ASME, SAE, and ASEE
Hartford, Connecticut, July 21–23, 2008

National Aeronautics and
Space Administration

Glenn Research Center
Cleveland, Ohio 44135

November 2008

This work was sponsored by the Fundamental Aeronautics Program at the NASA Glenn Research Center.

Level of Review: This material has been technically reviewed by technical management.

Available from

NASA Center for Aerospace Information
7115 Standard Drive
Hanover, MD 21076–1320

National Technical Information Service
5285 Port Royal Road
Springfield, VA 22161

Available electronically at http://gltrs.grc.nasa.gov

Preliminary Test Results of a Non-Contacting Finger Seal on a Herringbone-Grooved Rotor

Margaret P. Proctor and Irebert R. Delgado
National Aeronautics and Space Administration
Glenn Research Center
Cleveland, Ohio 44135

Abstract

Low leakage, non-contacting finger seals have potential to reduce gas turbine engine specific fuel consumption by 2 to 3 percent and to reduce direct operating costs by increasing the time between engine overhauls. A non-contacting finger seal with concentric lift-pads operating adjacent to a test rotor with herringbone grooves was statically tested at 300, 533, and 700 K inlet air temperatures at pressure differentials up to 576 kPa. Leakage flow factors were approximately 70 percent less than state-of-the-art labyrinth seals. Leakage rates are compared to first order predictions. Initial spin tests at 5000 rpm, 300 K inlet air temperature and pressure differentials to 241 kPa produced no measurable wear.

Nomenclature

A	seal leakage area, m^2
C	radial clearance, mm
C_d	discharge coefficient
D_1	bearing bore diameter, m
D_{seal}	outside diameter of the seal rotor, m
f	friction coefficient
M	Mach number
$\dot{m}$	air leakage flow rate, kg/s
P	air pressure downstream of seal, MPa
P_u	air pressure upstream of seal, MPa
R	gas constant, kJ/kg-K
T	bearing torque loss, N-m
T_{avg}	average seal air inlet temperature, K
T_u	upstream air temperature, K
W	load on bearing, N
ΔP	pressure drop across seal, kPa
Φ	flow factor, kg-$K^{1/2}$/MPa-m-s
γ	ratio of specific heats (1.4 for air)

I. Introduction

Low leakage seals have potential to reduce gas turbine fuel consumption by 2 to 3 percent and to reduce direct operating costs by increasing the time between engine overhauls (ref. 1). Fixed clearance labyrinth seals, used throughout gas turbine engines, have high leakage rates due to large clearances needed to avoid rubbing contact during engine operation but have long life capability. Labyrinth seals

used with abradable materials run with tighter clearances and have less leakage. However, as the abradable materials wear with time and during rotor excursions the clearances open and leakage rate increases. Brush and finger seals have leakage rates less than half that of labyrinth seals but are life limited due to rubbing contact (refs. 2 and 3). Furthermore, increasingly higher shaft speeds and operating temperatures required for advanced gas turbine engines are pushing the material capability limits of contacting seals. Alternatively, non-contacting, compliant seals have very small seal-to-rotor clearances, which minimize seal leakage rates and reduce specific fuel consumption and emissions. Compliant features allow this type of seal to accommodate thermal and centrifugal growth and shaft dynamic motion while maintaining seal clearance. This results in little to no wear and long life capability.

To investigate the potential of the non-contacting finger seal and to provide data to develop a verified design methodology for it, a baseline non-contacting finger seal was designed and fabricated. This NASA patented design (ref. 4) primarily differs from the Arora design patented by AlliedSignal (ref. 5) in that it eliminates the lift pads on the high pressure fingers. It was felt that hydrostatic pressures on the outer diameter (o.d.) of the lift pads would overwhelm any lift forces generated by them. Static performance tests at 300, 533, and 700 K inlet air temperatures at pressures up to 576 kPa and spin tests at 300 K, 5000 rpm and pressures up to 241 kPa were conducted. This paper presents the test hardware, apparatus, and experimental procedures used to test the baseline non-contacting finger seal against a herringbone-grooved rotor. It should be pointed out that unexpected findings prompted exploratory bind-up tests not typical of previous test procedures. The seal leakage performance, power loss, and wear results are presented and discussed.

II. Test Hardware

The baseline non-contacting finger seal is made of Haynes-188, a solid-solution-strengthened superalloy, for operations at temperatures up to 1089 K. It is comprised of a back plate, aft spacer, aft finger element, forward finger element, forward spacer and front plate as shown in figure 1. These components are held together with 20 flat head screws. Typical finger seals would be fastened together with rivets ground flush with the front and back plates. Also, the back plate would typically be about the same thickness as the front plate. This seal was designed with a much thicker back plate to accommodate fastening components with screws so that different finger elements could be tested without replacing all the individual seal components.

The forward finger element, also referred to as the high pressure finger element, is a washer made of thin sheet stock with multiple curved slots machined around the inner diameter (i.d.) to form the fingers. The aft finger element, or the low pressure finger element, is essentially the same as the forward finger element except that each finger has an axial extension at the seal inner diameter that forms a lift pad concentric to the rotor. The lift pad has a circumferential groove to insure low pressure on all edges of the lift pad. This can be seen in figure 2. The forward and aft finger elements are oriented to each other such that the fingers of each element block the slots in the other element. The fingers act as cantilever beams, flexing in response to rotor dynamic motion and radial growth of the rotor due to centrifugal and thermal forces. This compliant feature permits operation at clearances much smaller than fixed clearance seals resulting in lower leakage rates. Geometric features on the lift pad i.d. or on the rotor o.d. generate a hydrodynamic lift force during shaft rotation allowing the seal to ride on a thin film of air rather than rubbing against the rotor. While a non-contacting finger seal is expected to have slightly higher leakage than a contacting finger seal, it should have the benefit of low wear. The lift pads of the baseline non-contacting finger seal are concentric to the rotor o.d. Lift forces are generated during rotation by the herringbone-groove pattern on the rotor o.d.

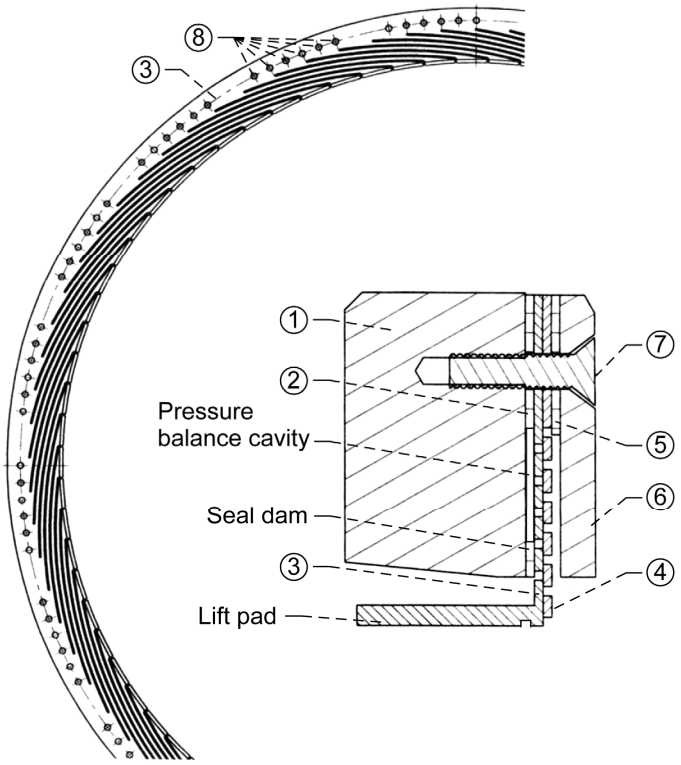

Figure 1.—Non-contacting finger seal design: 1, back plate; 2, aft spacer; 3, aft finger element; 4, forward finger element; 5, forward spacer; 6, front plate; 7, screw; 8, indexing and screw holes.

Figure 2.—Pre-test photo of non-contacting finger seal inner diameter.

Another difference between the forward and aft finger elements is that the high pressure finger element has an inner diameter that is 0.762 mm larger than the low pressure finger element. This was done to ensure that the high pressure finger element which has no lift pads would not touch the rotor due to pressure blow down effects. Applying a pressure differential across a finger seal generates a suction force that draws the fingers inwards towards the rotor due to the lower pressure under the finger pads. It may be possible to reduce the high pressure finger element inner diameter to match the low pressure

finger element if there is sufficient friction between the two elements to keep them moving together. Evidence that this is the case can be found in references 6, 7, and 8. The aft spacer forms the pressure balance cavity between the aft finger element, the back plate and seal dam. High pressure is fed to the balance cavity through a series of slots in the spacers and holes in the finger elements. The pressure balance cavity reduces the normal force, and hence the friction force, at the seal dam. This is essential to reducing hysteresis in the seal.

The 21.6-cm-diameter test rotor is made of Grainex MAR-M-247, a nickel-base alloy with excellent high-temperature properties. The seal runner surface on the rotor outer diameter is coated with chrome carbide applied by high-velocity oxygen fuel thermal spraying. A herringbone-groove pattern was machined into this coating by plunge electro-discharge machining. A pre-test photo of the grooves is shown in figure 3. The groove design geometry is shown in figure 4. The groove geometry and rotor surface finish was measured with a profilometer. The measured groove depth and land surface finish is 20 and 0.2 μm, respectively. The seal is positioned so that the lift pad rides over the herringbone-grooves with the groove ends beginning at the middle of the circumferential groove on the lift pad and extending past the low pressure edge. Based on the inspected inner diameter of the seal prior to machining the slots to create the fingers and the inspected rotor outer diameter, the radial clearance between the seal and the rotor at room temperature is 25.4 μm.

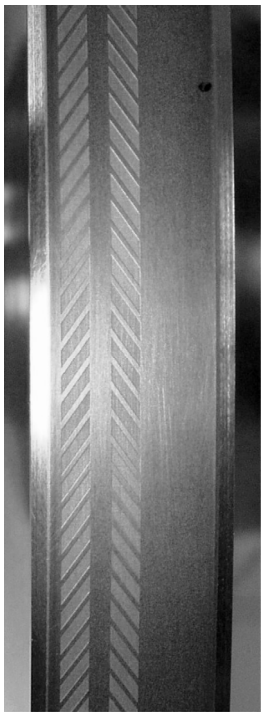

Figure 3.—Pre-test photo of herringbone grooves on seal test rotor.

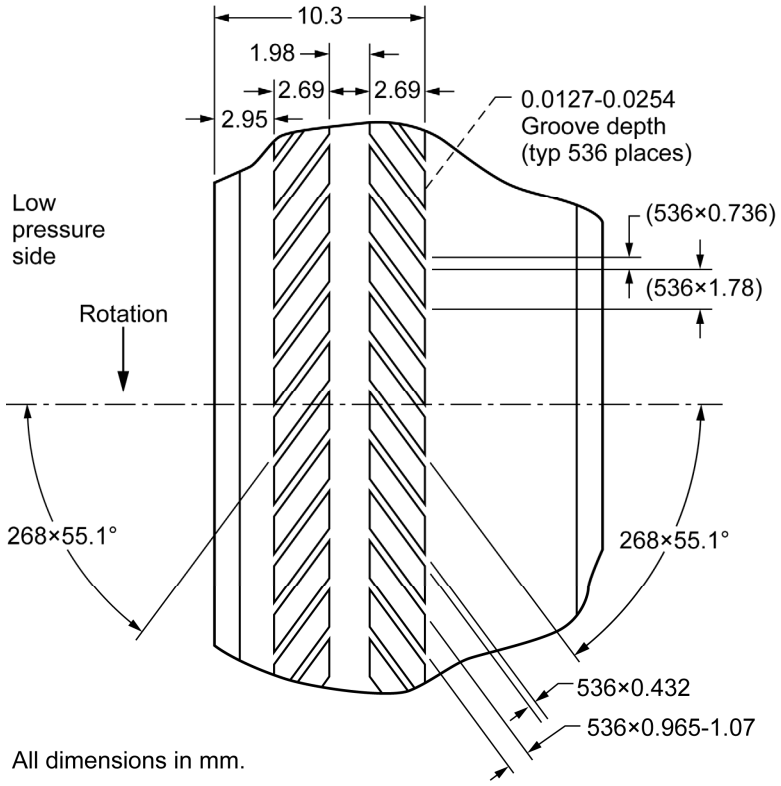

Figure 4.—Herringbone groove design.

III. Test Apparatus

A. Turbine Seal Test Rig

Testing was conducted in the NASA High-Temperature, High-Speed Turbine Seal Test Rig shown in figure 5 and located at the Glenn Research Center in Cleveland, Ohio. The turbine seal test rig consists of a 21.6-cm diameter test rotor mounted on a shaft in an overhung configuration. The shaft is supported by two oil-lubricated bearings. A balance piston controls the axial thrust load on the bearings due to pressure loads on the test rotor. An air turbine drives the test rig. A torquemeter is located between the air turbine and the test rig and is connected to each by a quill shaft. The test seal is clamped into the Grainex Mar-M-247 seal holder as shown in figure 6. A C-seal located at the seal holder/test seal interface prevents flow from bypassing the test seal at its outer diameter. The seal holder is heated to approximately match the thermal growth of the rotor and prevent a damaging change in radial clearance. Heated, filtered air enters the bottom of the test rig and passes through an inlet plenum that directs the heated air axially toward the seal-rotor interface. The hot air either leaks through the test seal to the seal exhaust line or exits the rig before the test seal through a controlled bypass line at the top of the rig. If seal leakage is low, the bypass line must be open to maintain sufficient flow through the test rig to keep the rig hot.

B. Instrumentation

Seal inlet and exit temperatures and static pressures, seal upstream metal temperature, and seal backface temperatures were measured at the locations shown in figure 6. For each measurement there were three probes equally spaced around the circumference, except for the upstream seal metal temperature for which two thermocouples were located at the 90° and 180° positions (0° is top dead center). Type-K thermocouples were used and all were 1.57 mm, Inconel sheath, closed ball except the seal exit temperatures, which were 3.2-mm diameter and the seal metal and backface temperatures, which were open-ball.

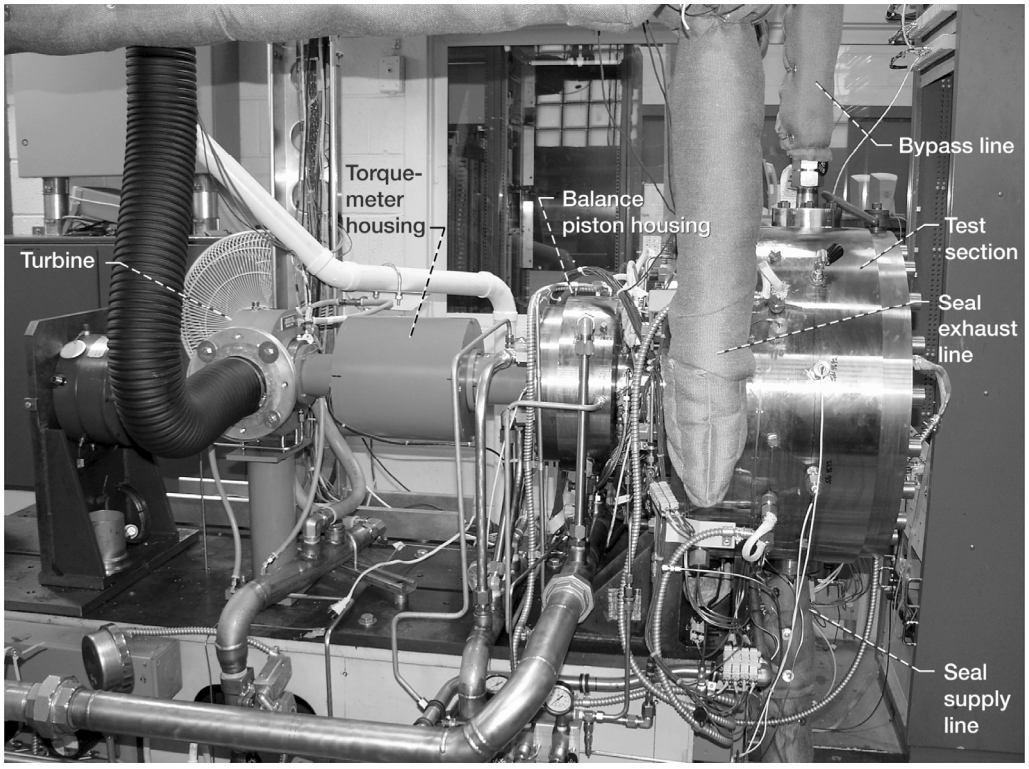

Figure 5.—High-temperature, high-speed turbine seal rig.

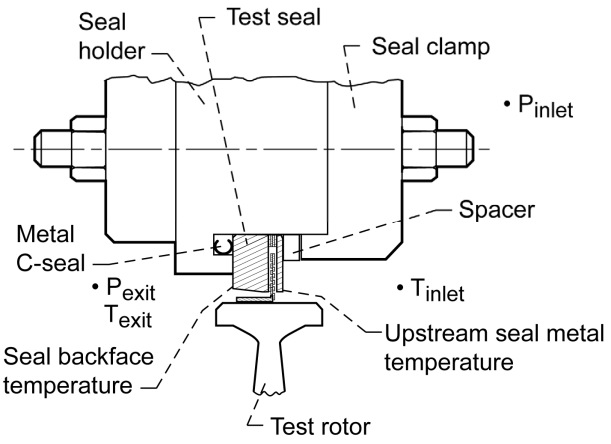

Figure 6.—Test seal configuration and location of research measurements.

Annubar (Rosemount, Inc.) flow meters are used to measure the flow rates of the hot air supplied to the rig and the air exiting the rig through the bypass line. The seal leakage is the difference between these two flow measurements. The seal leakage rate is then used to calculate the flow factor, which is defined as:

$$\Phi = \frac{\dot{m}\sqrt{T_{\text{avg}}}}{P_u \times D_{\text{seal}}} \tag{1}$$

The flow factor can be used to compare the leakage performance of seals with different diameters and with different operating conditions. The accuracy of the measured flow factor is ±1.5 percent.

A phase shift torquemeter measures the total torque of the seal test rig. It has a feature to compensate for any relative motion between the torsion shaft and stator. The torquemeter is rated to 22 N-m, has a maximum operating speed of 50,000 rpm, and an absolute accuracy of 0.13 percent or 0.028 N-m. The speed measurement from the torquemeter is accurate to <0.04 percent or 2 rpm at the maximum speed tested of 5000 rpm.

Seal power loss is simply the seal torque multiplied by speed. The seal torque is the total torque of the seal test rig with a seal installed minus the tare torque and the additional windage and bearing torques due to the pressure differential across the seal. The rig tare torque was measured at various inlet air temperatures and speeds with no seal installed. This data was two-dimensionally curve fitted. The fitted curve is used with the measured average inlet air temperature and speed to infer the corresponding tare torque. When a pressure differential is applied to the seal the windage from the high pressure side of the test disk and the balance piston increases due to the increased density of the air. In addition, the test end bearing experiences an additional axial load of 1334 N, which will increase the bearing windage beyond what is included in the measured tare torque. Windage error in the tare torque due to changes in oil viscosity is expected to be small since the bearing temperature variation between the seal tests and the tare test was very small. The additional windage on the high pressure side of the test disk and balance piston was calculated using an approximate solution from Schlichting (ref. 9). The additional torque from the higher axial load on the test end bearing was estimated using a friction coefficient of 0.0015 in equation (2) below:

$$T = fD_1\, W/2 \quad \text{(from ref. 10)} \tag{2}$$

Hence, the seal power loss presented is approximate.

IV. Experimental Procedures

A. Initial Static Tests

Initial static leakage performance tests were conducted at seal inlet air temperatures of 300, 533, and 700 K. At each inlet air temperature the pressure differential across the seal was increased incrementally from 0 to about 517 kPa or the maximum pressure differential that could be obtained. Then the pressure differential was incrementally decreased to 0 psid. Each condition was held for about 1 min while data was recorded. Data is recorded once per second and the data taken at a condition are then averaged together. This cycle was repeated one to three times. After the initial static leakage performance tests, it was discovered that the shaft was very difficult to turn by hand and was bound by the test seal. The seal was removed for visual inspection. The seal appeared the same as installed except for the inner diameter of the lift pads which were dark grey in color. Some of this color wiped off indicating possible contamination or oxidation. The seal was then reinstalled.

B. Bind-Up Tests

Next, a two part "bind-up" test was performed at room temperature to understand the conditions at which the seal would lock-up the shaft. To do this, the end cap on the turbine drive was removed to provide access to the drive shaft. In part one of the bind-up test, the pressure differential across the seal was increased from zero to the test pressure. The test pressure was held for approximately 1 min and then the pressure differential across the seal was reduced back to zero. Then a wrench was used on the drive shaft end to try turning the shaft by hand. This was done for test pressures of 69, 138, 207, 276, 345, 414, and 483 kPa. In all cases the shaft turned easily. In part two of the bind-up test, the pressure differential across the seal was increased in 13.8 kPa increments to 276 kPa and then increased to 483, 552, and 576 kPa. At each pressure condition a wrench was used to try turning the shaft by hand and to assess the relative ease of turning the shaft, except at 552 and 576 kPa. The shaft was turned at pressure differentials from 0 to 276 kPa. A decrease in ease of turning was first observed at 83 kPa, although the shaft turned easily enough to free wheel up to 193 kPa. The shaft became increasingly more difficult to turn. At 276 kPa the shaft was turned a tiny amount, but it was decided not to force turning the shaft to prevent damage to the seal or rotor coating. At 576 kPa, the shaft was bound very tight. When the pressure differential across the seal was reduced to 0 kPa the shaft turned easily by hand. As a result of this bind-up test, it was decided that dynamic testing at all test speeds should first be conducted at low pressure conditions up to 241 kPa. Then dynamic testing could be done at higher pressure differentials.

After the bind-up tests the seal was again removed for visual inspection. Scrapings of the dark grey deposit on the seal were taken and energy dispersive spectroscopy was performed on the samples. Then the seal was placed in a water and detergent bath and ultrasonically cleaned. After air drying, the seal was placed in an oven at 400 K for 1 hr to bake out any moisture between the laminates. The seal was weighed and compared to pre-test measurements it lost 0.3 grams.

C. Repeat Static Tests

Static leakage performance tests at seal inlet air temperatures of 300, 533, and 700 K were repeated. The pressure differential across the seal was incrementally increased and decreased from zero to maximum pressure to 0 kPa three times. On the third cycle, with the pressure differential increased to 13.8 kPa, the shaft was turned by hand about 10 times. After the rig had cooled, the rig cover plate was removed and the shaft could not be turned. Applying 11.3 N-m at the turbine drive end did not rotate the shaft. Again the seal clamp had to be loosened to loosen the seal from the shaft. The seal was removed and visually inspected. The seal's appearance was similar to what it was before this test. There was no change in seal weight. In addition, 16 of the low pressure lift pads were cocked axially away from the high pressure fingers. It appears that the high pressure fingers can not lay flat against the low pressure

fingers where the low pressure finger pads are axially cocked. This means that these high-pressure fingers likely cannot seal the gap between the low-pressure fingers with the cocked lift pads unless the fingers with the cocked lift pads move into proper position under pressure.

In retrospect, the fact that the seal locked up the shaft makes sense given that the pressure differential across the seal during cooling was 345 kPa. We know from the bind-up tests that at pressures above 276 kPa the seal grabs the shaft. We also know that at higher temperatures the radial clearance between the shaft and seal increases due to the difference in the coefficients of thermal expansion. So as the rig cools while the seal is locked onto the shaft, the radial clearance decreases and captures the seal in the locked-up position.

D. Spin Tests

The seal was reinstalled and the initial room temperature spin test was conducted. First the pressure differential across the seal was set to 13.8 kPa. Then the shaft speed was quickly increased to 5000 rpm. At this speed data was recorded at pressure differentials of 13.8, 34, 69, 103, 138, 103, 69, 34, and 13.8 kPa. After the shaft stopped rotating the pressure differential across the seal was brought to zero and the test concluded. This procedure is followed because it is important to have some cooling flow to the seal in the event that rubbing contact occurs. For this test two thermocouples were installed to measure the seal front cover plate metal temperature at the 90° and 270° locations. After this initial spin test the seal was removed for visual inspection and found to be in good condition. There was no significant change in seal weight after 25 min of rotational testing.

The seal was re-installed. A single cycle leakage performance test was conducted at room temperature. Then a second spin test was conducted in the same manner as the first except the pressure was increased up to 241 kPa. The time of rotational operation in this second spin test was 68 min. A total of 93 min of rotational testing were accumulated in the first and second spin tests combined. Again, after the second spin test, the seal was removed for visual inspection and weighed. The seal was found to be in good condition and its weight was the same.

V. Leakage Flow Model

A simple leakage flow model was used to predict the seal leakage rate. There are three flow paths for air to leak through the seal as illustrated in figure 7. The first flow path goes from high pressure through the slots in the spacers and holes in the finger elements into the pressure balance cavity and then exits through the finger slots at the seal dam. The second flow path goes through the pinholes created by the high pressure finger element i.d., the rotor o.d., and the circumferential gaps between the lift pads. The third flow path goes under the lift pads. The sum of the areas for each of these three flow paths equals the seal leakage area. The leakage rate through the seal is predicted using the isentropic flow equation as shown in equation (3). A discharge coefficient of 0.65, which is typical of orifices, can be applied to account for inlet and exit losses.

$$\dot{m} = \frac{P_u}{\sqrt{RT_u}} \cdot A\sqrt{\gamma} M \left(1 + \left(\frac{\gamma - 1}{2}\right) M^2\right)^{1/2 - \frac{\gamma}{\gamma - 1}} \tag{3}$$

Where

$$M = \left[\left(\left(\frac{P_u}{P}\right)^{\frac{\gamma - 1}{\gamma}} - 1\right)\frac{2}{\gamma - 1}\right]^{\frac{1}{2}} \tag{4}$$

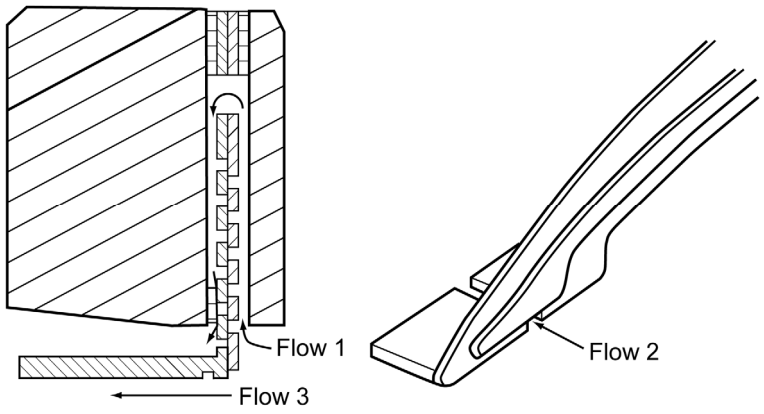

Figure 7.—Leakage flow paths included in non-contacting finger seal flow model.

For air ($\gamma = 1.4$), when the pressure ratio, $P/P_{u,} \leq 0.5283$, the flow is choked and equation (3) reduces to

$$\dot{m} = \frac{P_u}{\sqrt{RT_u}} \cdot A \cdot (0.6847) \tag{5}$$

This simple model is based on several assumptions beyond the assumption of isentropic flow. It is assumed that the geometry is fixed, that the lift pads remain concentric to the rotor, and that the finger elements are held firmly against each other and the seal dam so that there is no leakage between the contacting areas. While it may seem odd to assume a fixed geometry for a compliant seal, the seal radial clearance is an input parameter. Also, for the seal tested, the flow area of the finger slots at the seal dam is approximately eleven times smaller than the flow restrictions upstream of it. Therefore, these finger slots control the leakage flow rate in this path and it can be safely assumed that the pressure in the balance cavity is equal to the seal inlet pressure.

VI. Seal Performance

A. Leakage

The initial static leakage performance of the non-contacting finger seal at inlet air temperatures of 300 K is shown in figure 8. The maximum flow factor of approximately 17.4 kg-$K^{1/2}$/MPa-m-s occurred at approximately 428 kPa across the seal. The data show little hysteresis after the first cycle of increasing pressure differential.

The initial static leakage performance at inlet air temperatures of 533 and 700 K are shown in figures 9 and 10, respectively. At these conditions the seal exhibits much more hysteresis than at room temperature. In all cycles the flow factor is lower for decreasing pressure differential than for increasing pressure differential. The maximum flow factor occurred at 283 kPa and was 22.7 and 24.5 kg-$K^{1/2}$/MPa-m-s for 533 and 700 K, respectively. These higher flow factors can be attributed to an increase in radial clearance between the rotor and seal due to the difference in the coefficients of thermal expansion for the seal and rotor materials. At room temperature the radial clearance is 25.4 μm. Assuming the rotor and seal are both at 533 K the radial clearance increases to 48.3 μm, nearly double the build clearance. At 700 K the radial clearance grows to 61 μm.

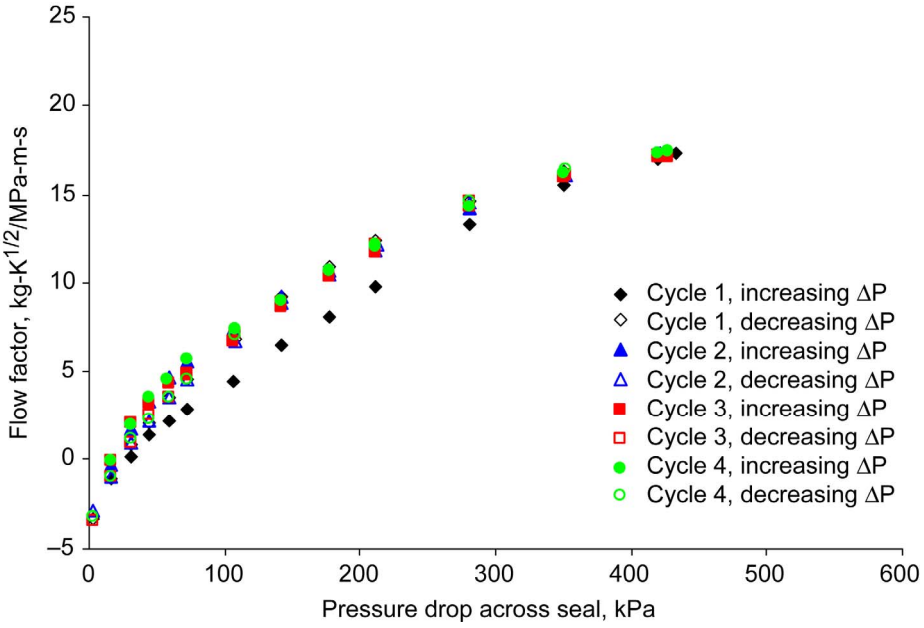

Figure 8.—Initial static leakage performance at 300 K.

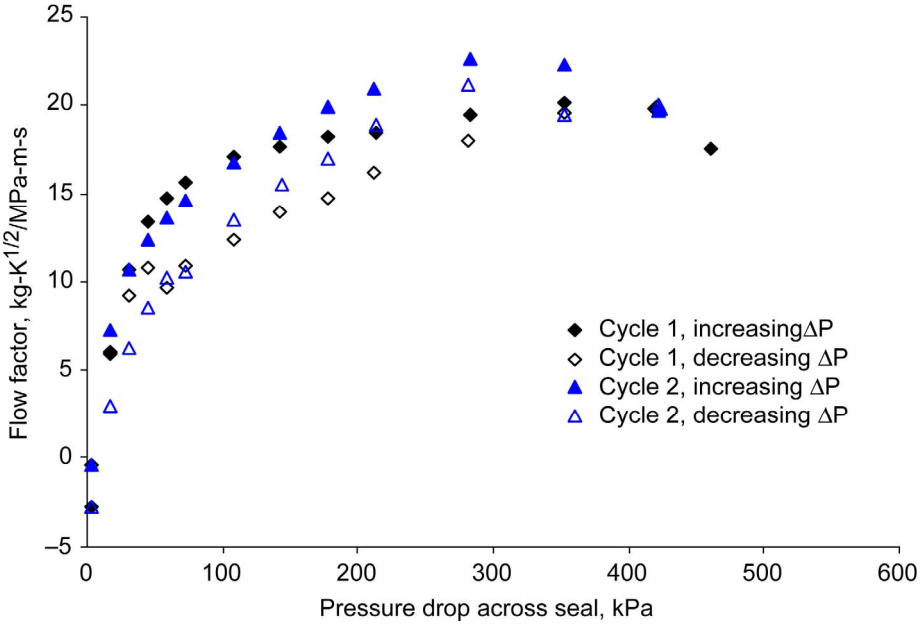

Figure 9.—Initial static leakage performance at 533 K.

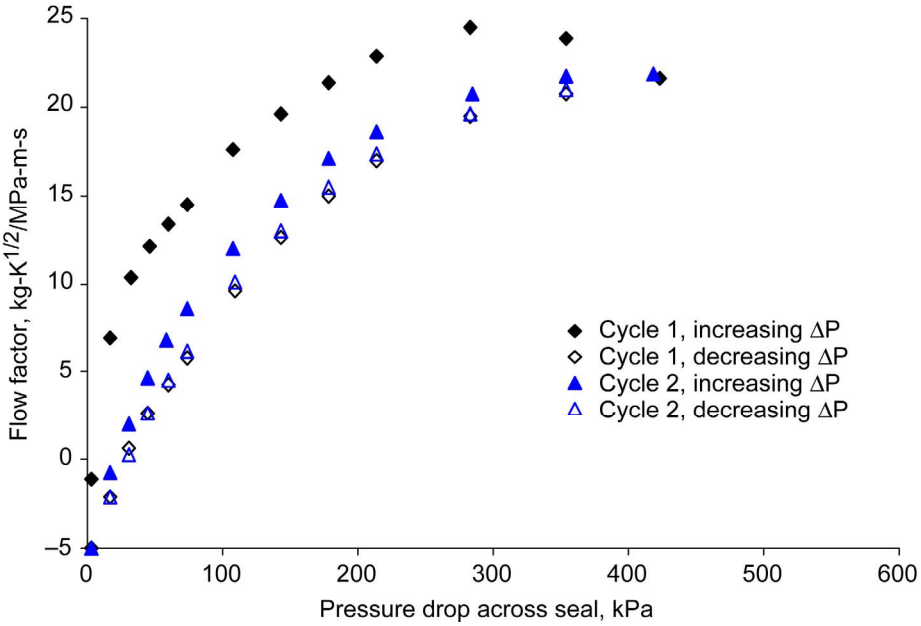

Figure 10.—Initial static leakage performance at 700 K.

The static leakage performance of the seal measured during parts 1 and 2 of the bind-up test are shown in figures 11 and 12, respectively. In part 1 of the test the inlet air temperature steadily increased from 320 to 344 K due to residual heat in the insulated piping between the air heater and the test rig. The maximum flow factor was 13.8 kg-$K^{1/2}$/MPa-m-s at 421 kPa which is less than the initial static leakage test. Recall that the shaft is turned by hand at 0 kPa between each data point. Rotation assists in moving the seal into its optimum position. In part two of the bind-up test the inlet air temperature was 342 to 345 K. The maximum flow factor in part 2 of the bind-up test was 9.77 kg-$K^{1/2}$/MPa-m-s at 585 kPa and is lower than the flow factor in part 1 of the bind-up test. Recall that in part 2 of the bind up test that the shaft is rotated by hand at every pressure differential test point up to 276 kPa. This result further demonstrates the importance of shaft rotation to obtaining the optimum seal position.

The repeat static test seal leakage performance at 300 K is shown in figure 13. The maximum flow factor ranges between 10.3 and 13.2 kg-$K^{1/2}$/MPa-m-s at the pressure differentials of 420 to 467 kPa, which is about 24 to 41 percent less than in the initial test. Further, this flow factor is approximately 64.4 to 82.5 percent of the flow factor of 16.0 kg-$K^{1/2}$/MPa-m-s for a straight 4-tooth labyrinth seal with a radial clearance of 229 μm (ref 11). Unlike the initial static test at 300 K in figure 8, there is quite a bit of hysteresis. In all cycles the flow factor is lower for decreasing pressure differential than for increasing pressure differential. Since there are no temperature changes, the hysteresis most likely is due to internal friction forces within the seal. As pressure differential increases the fingers move towards the rotor due to the pressure blow down effect. It is surmised that friction forces hold the fingers at the smaller clearance as pressure differential decreases resulting in a lower flow factor. Reducing the pressure differential to zero releases the fingers. In comparison to initial tests the repeat static tests at 533 and 700 K had similar hysteresis and 10 to 20 percent lower maximum flow factors.

For a fixed clearance seal, choked flow is evidenced by a constant flow factor at increasing pressure differentials. In air, choked flow should occur at a downstream to upstream pressure ratio of 0.5283, which corresponds to a pressure differential of 90 kPa for a downstream pressure of 101 kPa. Choked flow occurred very close to this pressure differential in previous tests with labyrinth and brush seals (ref 11). This means that the seal exit pressure taps are properly located. Further, since the flow factor does not level out at 90 kPa the data for the non-contacting finger seal indicate that the leakage area is increasing with increasing pressure differential until 345 to 414 kPa.

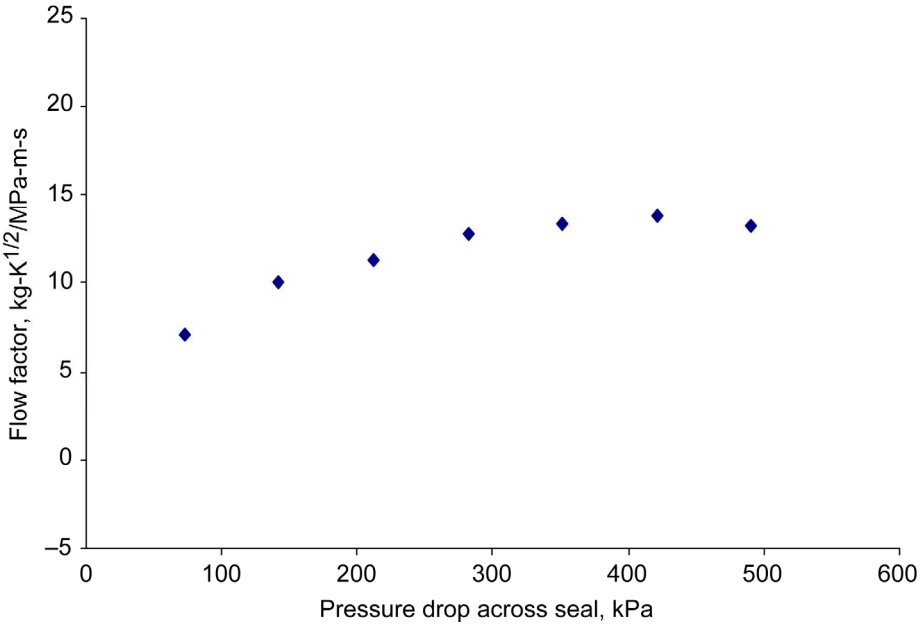

Figure 11.—Bind-up test part 1 static leakage performance at 320 to 344 K.

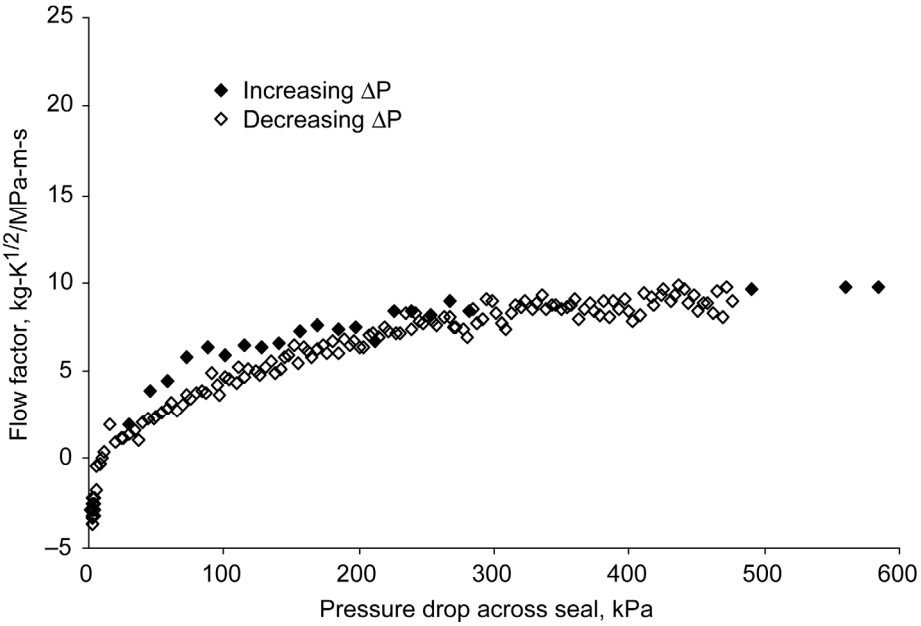

Figure 12.—Bind-up test part 2 static leakage performance at 342 to 345 K.

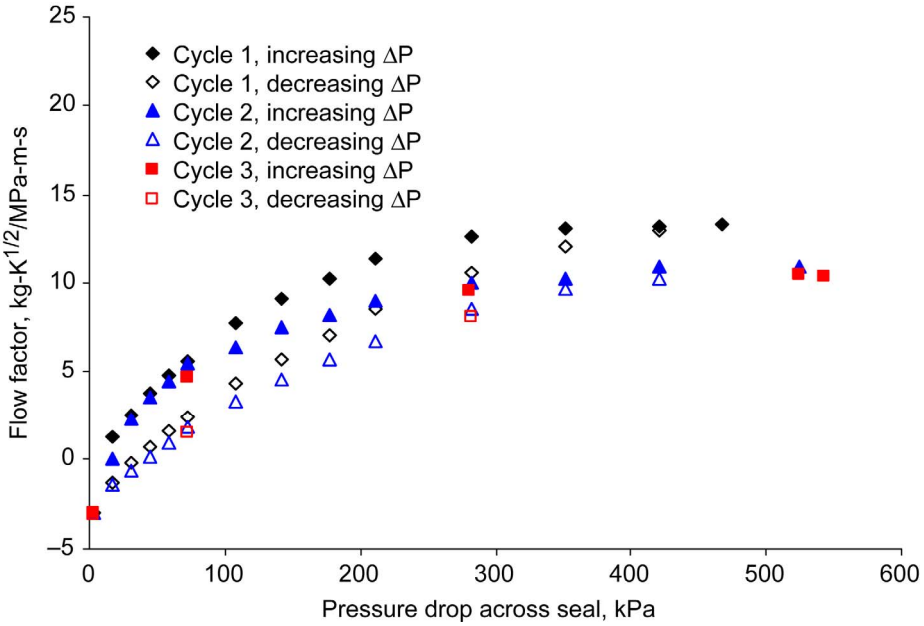

Figure 13.—Repeat static test leakage performance at 300 K.

The leakage performance of the non-contacting finger seal just prior to and during the second spin test at 5000 rpm is shown in figure 14. The predicted flow factors are also shown and are in reasonable agreement with the data. Hysteresis is present in both the static and second spin test data. However, the flow factor with shaft rotation at 5000 rpm is substantially less than the static flow factor, approximately half at 241 kPa where it begins to level out. The measured flow factor at 5000 rpm and 241 kPa was 5.2 kg-$K^{1/2}$/MPa-m-s. This is less than one third of the measured flow factor of a straight four-tooth labyrinth seal and less than one half the flow factor of a contacting brush seal at static conditions reported in reference 11. The measured flow factor for the non-contacting finger seal at 56 m/s (5000 rpm), 296 K, and 241 kPa is similar to that measured for a contacting finger seal at 186 m/s, 700 K and 276 kPa of 3 to 6 kg-$K^{1/2}$/MPa-m-s reported in reference 12.

B. Power Loss

The seal power loss at 5000 rpm and room temperature conditions is shown in figure 15 and increases as a function of pressure drop across the seal. The maximum seal power loss at 5000 rpm is approximately 0.4 kW at 247 kPa. The seal exhibits some hysteresis, with seal power loss for decreasing pressure differentials approximately 30 percent less than for increasing pressure differentials. This hysteresis corresponds to that seen in the flow factor (fig. 14). This makes sense since lower flow factors indicate smaller clearances. Power loss decreases as radial clearance decreases (ref. 12). Although a direct comparison can not yet be made with the small amount of data obtained, it is observed that the non-contacting seal power loss is of the same order of magnitude as that for contacting brush and finger seals (refs. 11 and 12).

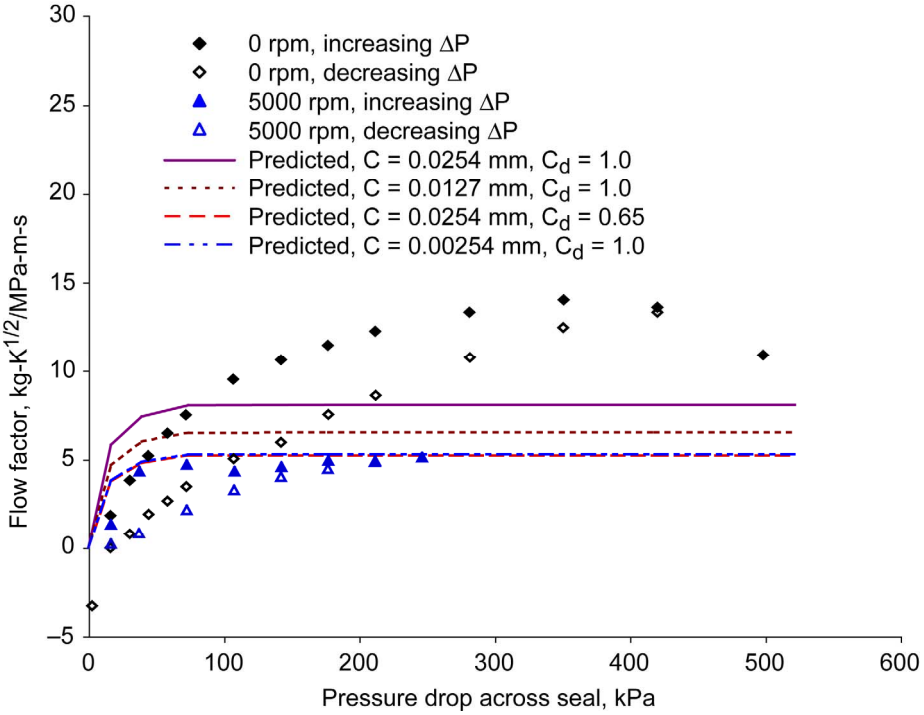

Figure 14.—Second spin test leakage performance at 300 K.

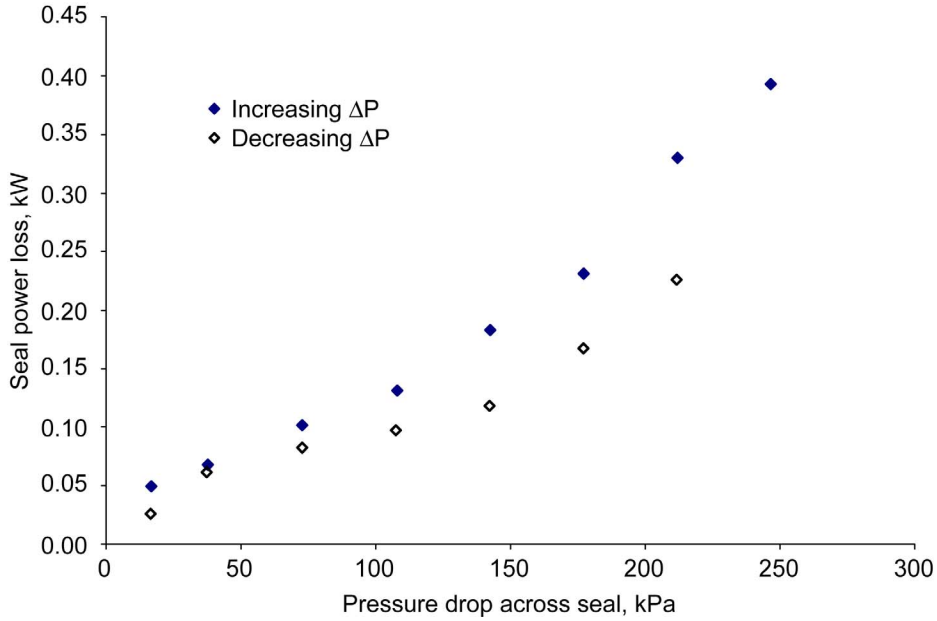

Figure 15.—Second spin test seal power loss at 300 K.

VII. Wear Results

After the initial spin test the seal was removed for visual inspection and found to be in good condition. There was no significant change in seal weight. All the low pressure lift pads have a hint of burnishing on the inner diameter near the high pressure edge. Some pads have this burnishing over the entire circumferential length and others just near a corner. This burnishing did not have any depth perceptible by touch. The inner diameters of the high pressure fingers have a small burnished (shiny) area at the finger toe. All fingers and lift pads are free to move radially inward when lightly touched. The rotor outer diameter was visually inspected using a mirror. It had a shiny track of even axial length around the entire circumference, which appeared to be the same axial length as the burnished areas on the seal. There is no distinguishable depth by touch. The grooves appeared clean and free of debris. Visual inspection of the seal and rotor after the second spin test found no changes. The seal weight did not change either. Given the good condition of the seal and rotor it is concluded that non-contacting operation was achieved. The burnishing is likely the result of brief rubbing contact while starting and stopping shaft rotation. The absence of a rapid and substantial rise of the seal exit and back face temperatures further substantiates this conclusion.

VIII. Conclusions

Based on this preliminary data the non-contacting finger seal holds promise to achieve both low leakage and long life capability for the following reasons:

1. After 93 min of rotation at 300 K and 5000 rpm there was no measurable wear.
2. Non-contacting operation was achieved at 5000 rpm at pressures from 14 to 241 kPa.
3. The measured flow factor of this non-contacting finger seal at 5000 rpm and 241 kPa was less than one third of the measured flow factor of a straight four-tooth labyrinth seal and less than one half of the measured flow factor of a contacting brush seal at static conditions.
4. Rotation is required to properly seat the seal and results in lower flow factors.
5. Non-contacting finger seal power loss is the same order of magnitude as brush and finger seals.

Although the simplified leakage model is in reasonable agreement with the measured flow factors once the flow chokes, further analysis and testing is needed to fully understand the nuances of this particular non-contacting finger seal design and to develop useful design methodologies and predictive tools. Fluid-structural modeling of the seal is needed to understand the bind-up observed at pressures greater than 276 kPa and to determine design modifications to achieve higher pressure capability.

References

1. Steinetz, B.M., Hendricks, R.C., and Munson, J., “Advanced Seal Technology Role in Meeting Next Generation Turbine Engine Goals,” NASA/TM—1998-206961, April 1998.
2. Arora, G.K., Proctor, M.P., Steinetz, B.M., and Delgado, I.R., “Pressure Balanced, Low Hysteresis, Finger Seal Test Results,” NASA/TM—1999-209191, June 1999; also AIAA Paper 99–2686, June 1999.
3. Arora, G.K., and Proctor, M.P., “JTAGG II Brush Seal Test Results,” NASA TM 107448, July 1997; also AIAA paper 97–2632, July 1997.
4. Proctor, M.P. and Steinetz, B.M., U.S. Patent for “Non-Contacting Finger Seal,” Patent No. US 6,811,154 B2, Nov. 2, 2004.
5. Arora, G.K., U.S. Patent for “Non-Contacting Finger Seal With Hydrodynamic Foot Portion,” Patent No. 5,755,445, May 26, 1998.
6. Braun, M.J., Deng, D.F., Pierson, H.M., Proctor, M.P., and Steinetz, B.M., “A Three Dimensional Thermofluid Analysis and Simulation of Flow, Temperature, and Pressure Patterns in a Passive-

Adaptive Compliant Finger Seal," The 10th International Symposium on Transport Phenomena and Dynamics of Rotating Machinery, Honolulu, HI, March 7–11, 2004, ISROMAC10–2004–126.
7. Braun, M.J., Pierson, H.M., Deng, D.F., Choy, F.K., Proctor, M.P., and Steinetz, B.M., "Structural and Dynamic Considerations Towards the Design of a Padded Finger Seal," 39th AIAA/ASME/SAE/ASEE Joint Propulsion Conference, Huntsville, AL, July 20–23, 2003, AIAA–2003–4698.
8. Marie, H., "A Study of Non-Contacting Passive-Adaptive Turbine Finger Seal Performance, Volume 1," PhD Dissertation, University of Akron, Akron, OH, 2005.
9. Schlichting, H., 1979, Boundary Layer Theory, 7th edition, McGraw-Hill, Inc., New York, NY, pp. 242–243.
10. Townsend, D.P., Editor in Chief, 1991, Dudley's Gear Handbook, 2nd edition, McGraw-Hill, Inc., New York, NY, pp. 12.17–12.24.
11. Proctor, M.P., and Delgado, I.R., "Leakage and Power Loss Test Results for Competing Turbine Engine Seals," NASA/TM—2004-213049, May 2004.
12. Delgado, I.R., and Proctor, M.P., "Continued Investigation of Leakage and Power Loss Test Results for Competing Turbine Engine Seals," NASA/TM—2006-214420, Sept. 2006.

REPORT DOCUMENTATION PAGE	Form Approved OMB No. 0704-0188

1. REPORT DATE *(DD-MM-YYYY)*	2. REPORT TYPE	3. DATES COVERED *(From - To)*
01-11-2008	Technical Memorandum	

4. TITLE AND SUBTITLE
Preliminary Test Results of a Non-Contacting Finger Seal on a Herringbone-Grooved Rotor

5a. CONTRACT NUMBER

5b. GRANT NUMBER

5c. PROGRAM ELEMENT NUMBER

6. AUTHOR(S)
Proctor, Margaret, P.; Delgado, Irebert, R.

5d. PROJECT NUMBER

5e. TASK NUMBER

5f. WORK UNIT NUMBER
WBS 561581.02.08.03.15.02

7. PERFORMING ORGANIZATION NAME(S) AND ADDRESS(ES)
National Aeronautics and Space Administration
John H. Glenn Research Center at Lewis Field
Cleveland, Ohio 44135-3191

8. PERFORMING ORGANIZATION REPORT NUMBER
E-16560-1

9. SPONSORING/MONITORING AGENCY NAME(S) AND ADDRESS(ES)
National Aeronautics and Space Administration
Washington, DC 20546-0001

10. SPONSORING/MONITORS ACRONYM(S)
NASA

11. SPONSORING/MONITORING REPORT NUMBER
NASA/TM-2008-215475

12. DISTRIBUTION/AVAILABILITY STATEMENT
Unclassified-Unlimited
Subject Categories: 07 and 34
Available electronically at http://gltrs.grc.nasa.gov
This publication is available from the NASA Center for AeroSpace Information, 301-621-0390

13. SUPPLEMENTARY NOTES

14. ABSTRACT
Low leakage, non-contacting finger seals have potential to reduce gas turbine engine specific fuel consumption by 2 to 3 percent and to reduce direct operating costs by increasing the time between engine overhauls. A non-contacting finger seal with concentric lift-pads operating adjacent to a test rotor with herringbone grooves was statically tested at 300, 533, and 700 K inlet air temperatures at pressure differentials up to 576 kPa. Leakage flow factors were approximately 70 percent less than state-of-the-art labyrinth seals. Leakage rates are compared to first order predictions. Initial spin tests at 5000 rpm, 300 K inlet air temperature and pressure differentials to 241 kPa produced no measurable wear.

15. SUBJECT TERMS
Seals; Finger seal; Leakage; Power loss; Performance; Brush seal

16. SECURITY CLASSIFICATION OF:			17. LIMITATION OF ABSTRACT	18. NUMBER OF PAGES	19a. NAME OF RESPONSIBLE PERSON
a. REPORT	b. ABSTRACT	c. THIS PAGE			STI Help Desk (email:help@sti.nasa.gov)
U	U	U	UU	22	19b. TELEPHONE NUMBER *(include area code)* 301-621-0390